

# First-principles study of the structure of methanethiolate on Ag(111)

Guo-min He

*Department of Physics, Xiamen University, Xiamen 361005, China*

(Received 10 March 2006; revised manuscript received 3 September 2006; published 18 December 2006)

We have systematically investigated the adsorption of methanethiolate ( $\text{CH}_3\text{S}$ ) on the Ag(111) surface employing density-functional theory. Various adsorption geometries have been considered and the energetically most favorable structure of  $\text{CH}_3\text{S}/\text{Ag}(111)$  was identified. Though the calculated structural parameters for the layer spacing of the adsorbate relative to the nearest Ag layer and the S-Ag bond lengths are reasonable consistent with the experimental results, difference exists about the height corrugation in the S layer. Our results show that the buckling of the S layer observed in experiment might not represent the true atomic positions.

DOI: [10.1103/PhysRevB.74.245421](https://doi.org/10.1103/PhysRevB.74.245421)

PACS number(s): 68.43.-h, 71.15.Mb

## I. INTRODUCTION

Self-assembled monolayers (SAMs) of organic molecules on metal surfaces<sup>1,2</sup> have attracted much attention for their potential applications in many areas, such as molecular electronic devices, functionalization of metal surfaces, chemical sensors, and biocompatible coatings. For a SAMs system it generally consists of two parts: the molecule-substrate interface where the molecules interact with the substrate through a headgroup, and a chain part that constitutes the outer surface of the molecular layer. Accordingly, two types of interactions are involved: the molecule and substrate interaction in the interface region, and the intermolecular interaction between the chain parts. In general, the detailed structure of the molecule-metal interface is determined by a balance between these interactions. Knowledge of the molecule-metal interface structure is relevant to understanding these interactions which are indispensable for understanding the self-assembled mechanisms and the electronic properties of SAMs. Therefore, a few studies have been performed recently with the aim to establishing the detailed structure of the molecule-metal interface. For example, the structure of  $(\sqrt{3} \times \sqrt{3})\text{-CH}_3\text{S}/\text{Au}(111)$  phase has been studied by photoelectron diffraction<sup>3</sup> and x-ray standing wave.<sup>4</sup> It was found that  $\text{CH}_3\text{S}$  is located at the top sites. For the case of  $\text{CH}_3\text{S}/\text{Cu}(111)$  system, high-resolution photoelectron spectroscopy, x-ray standing wave and scanning tunneling microscopy (STM) studies<sup>5-7</sup> suggested the coexistence of low- and high-temperature thiolate phases in addition to an atomic sulfur phase at room temperature.

Recently, an experimental analysis using STM and low-energy electronic diffraction (LEED) has been performed on the  $\text{CH}_3\text{S}/\text{Ag}(111)$  surface.<sup>8</sup> It was found that an ordered methanethiolate structure was formed on the Ag(111) surface by reaction with dimethyl-disulfide ( $\text{CH}_3\text{S-SCH}_3$ ) at the room temperature. Some special features have also been demonstrated for the  $\text{CH}_3\text{S}/\text{Ag}(111)$  surface: (i) Distinctly different from the  $(\sqrt{3} \times \sqrt{3})\text{-CH}_3\text{S}/\text{Au}(111)$  phase, a well-ordered  $(\sqrt{7} \times \sqrt{7})\text{R}19^\circ\text{-CH}_3\text{S}/\text{Ag}(111)$  structure was observed. For such phase it consists of three distinctly different S sites relative to the underlying Ag substrate which were shown as corresponding to the top, hexagonal close packed (hcp), and fcc hollow sites. This is rather surprising because

for most simple adsorbates on the fcc(111) surfaces there are large energy differences between the top and two inequivalent hollow sites. (ii) The STM images provided evidence that  $\text{CH}_3\text{S}$  causes the surface Ag layer to reconstruct. For atomic adsorbates, it is a well-known phenomenon that adsorption induced surface rearrangement can occur. It is relatively unexplored involving a molecular adsorbate. (iii) The STM images also showed that there is a height variation for  $\text{CH}_3\text{S}$  at different adsorption sites which is about 0.3 Å, though there is no simple direct correlation between the height variations in the STM images and in the true atomic positions. In order to obtain the quantitative information on the interface structure of the  $(\sqrt{7} \times \sqrt{7})\text{R}19^\circ\text{-CH}_3\text{S}/\text{Ag}(111)$  surface phase, further investigation has been performed by normal-incidence x-ray standing wave (NIXSW) analysis.<sup>9</sup> The main results are as follows. (i) The resulting NIXSW structural parameter values clearly excluded any adsorption model on the clean Ag(111) surface (i.e., without reconstruction). (ii) A reconstructed surface model was proposed that comprises a near-hexagonal Ag surface layer with an Ag density of only 3/7 that of the underlying substrate layers, and all the  $\text{CH}_3\text{S}$  molecules are adsorbed into the hollow sites of the reconstructed Ag layer which correspond to the top, fcc, and hcp sites relative to the underlying unreconstructed substrate. Though the proposed model is consistent with the NIXSW measurements and with the STM observation, the question still remains because the reconstructed Ag layer is planar, all the  $\text{CH}_3\text{S}$  molecules are expected to have the same layer spacing to the Ag substrate. This is inconsistent with the experimental results because the corrugation of the S layer was suggested to be about 0.3 ~ 0.5 Å by the NIXSW measurement.

In contrast, theoretical studies of  $\text{CH}_3\text{S}$  on the Ag surface are rather limited. Virtually little is known about how  $\text{CH}_3\text{S}$  is incorporated at the surface and formed the SAMs' structure. To our knowledge, only a few theoretical studies of  $\text{CH}_3\text{S}/\text{Ag}(111)$  SAMs exist.<sup>10-12</sup> In these studies  $\text{CH}_3\text{S}$  adsorption on the Ag(111) surface was modeled by a two-layer thick closest-packed cluster or by a slab with four metal layers. However, the interface structure of  $\text{CH}_3\text{S}/\text{Ag}(111)$  has not been studied. Though some features of the interface structure have been revealed by experiment,<sup>8,9</sup> the detailed interface structure of  $\text{CH}_3\text{S}/\text{Ag}(111)$  still remains controver-

sial. In order to better understanding these issues we have studied the adsorption of  $\text{CH}_3\text{S}$  on the  $\text{Ag}(111)$  surface employing density-functional theory. In the present work we focus mainly on the interaction of  $\text{CH}_3\text{S}$  with the  $\text{Ag}(111)$  surface for various  $\text{CH}_3\text{S}$  adsorption geometries as a first step towards the understanding of the  $\text{CH}_3\text{S}/\text{Ag}(111)$  interface structure. The adsorption of  $\text{CH}_3\text{S}$  on the Ag surface is also of fundamental interest in relation to understanding these SAMs more generally.

This paper is organized as follows. The calculation method is given in Sec. II. Section III presents the calculated results. Finally, a brief summary is given in Sec. IV.

## II. METHOD OF CALCULATION

The density-functional theory total-energy calculations were performed with the SIESTA code (Ref. 13) within the local-density approximation (LDA). The Ceperley-Alder form of exchange and correlation energy function was used. The ion and core electrons were replaced by norm conserving pseudopotentials in their fully separable form, and numerical atomic orbitals were used as the basis sets.<sup>14</sup> We chose double  $\zeta$  atomic orbitals plus polarization orbitals as the basis sets with an equivalent plane-wave cutoff of 180 Ry to represent the charge density.

The surface is modeled by a four-layer slab separated by an 18-Å vacuum space and  $\text{CH}_3\text{S}$  is placed on one side of the slab. The positions of the top two Ag layers and the  $\text{CH}_3\text{S}$  molecules were allowed to relax until the forces were less than 0.03 eV/Å, while the bottom two layers of Ag were held fixed in their bulk positions. In the  $(1 \times 1)$  surface unit cell, more than 38 special  $k$  points were used in the surface irreducible Brillouin zone for the Brillouin-zone integration.

The stability of various  $\text{CH}_3\text{S}/\text{Ag}(111)$  structures is analyzed with respect to the adsorption energy. The adsorption energy is defined as<sup>15</sup>

$$E_{\text{ads}} = \frac{1}{n} [E_{n\text{CH}_3\text{S}/\text{Ag}}^{\text{slab}} - E_{n\text{CH}_3\text{S}} - E_{\text{Ag}}^{\text{slab}}], \quad (1)$$

where  $n$  is the number of the adsorbed molecules, and  $E_{n\text{CH}_3\text{S}/\text{Ag}}^{\text{slab}}$  is the total energy of the  $\text{CH}_3\text{S}/\text{Ag}(111)$  surface under consideration, while  $E_{n\text{CH}_3\text{S}}$  is the total energy of  $n$   $\text{CH}_3\text{S}$  gas-phase molecules which used the same geometries of the adsorbed molecules—i.e., without optimization, and spin-polarization was used.  $E_{\text{Ag}}^{\text{slab}}$  is the total energy of the reference system—i.e., the clean surface for the unreconstructed model and reconstructed surface for the reconstructed model. Note that (i) the energy required to form the reconstructed  $\text{Ag}(111)$  surface is not included and (ii) the error due to the basis set superposition error (BSSE) has been corrected by the counterpoise corrections—i.e., the same basis set as the total system  $n\text{CH}_3\text{S}/\text{Ag}(111)$  has been used to calculate the total energies of the separate substrate  $E_{\text{Ag}}^{\text{slab}}$  and adsorbate  $E_{n\text{CH}_3\text{S}}$ .<sup>16–18</sup> According to the definition,  $E_{\text{ads}}$  can be regarded as the energy required to separate the adsorbed system  $\text{CH}_3\text{S}/\text{Ag}(111)$  into two noninteracting parts: the  $\text{Ag}(111)$  surface and  $n$   $\text{CH}_3\text{S}$  molecules.

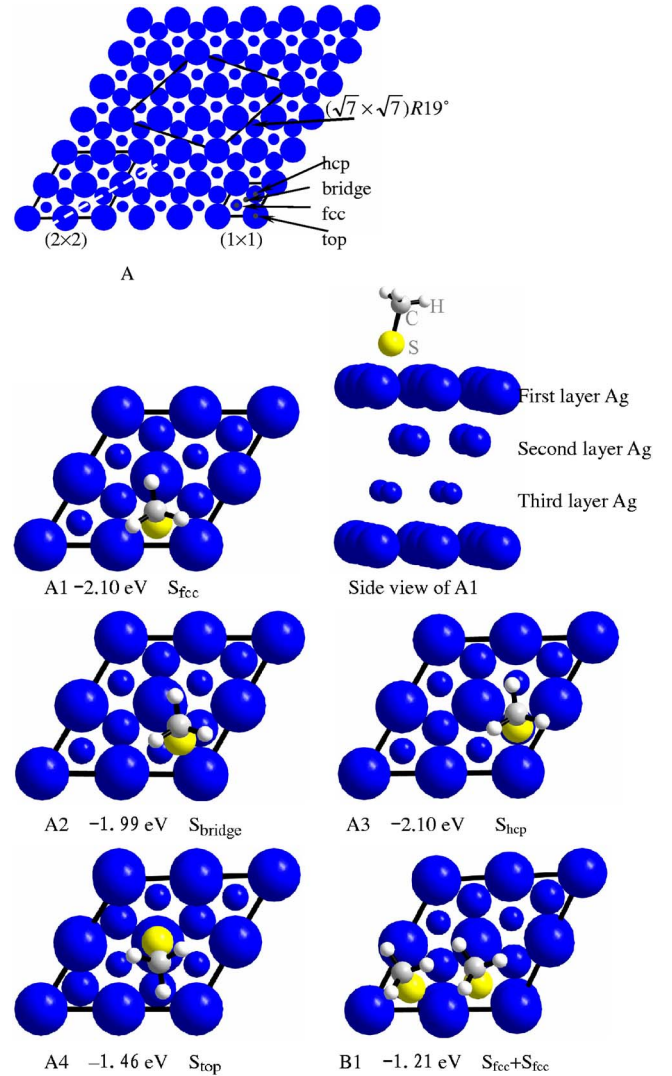


FIG. 1. (Color online) (A) Top view of the  $\text{Ag}(111)$  surface. The large, middle, and small circles denote the first layer, second layer, and third layer Ag atoms. The  $(1 \times 1)$ ,  $(2 \times 2)$ , and  $(\sqrt{7} \times \sqrt{7})R19^\circ$  surface unit cells were also indicated. The adsorption sites were represented by the small black dots. The dashed line indicates the studied path. (A1)–(B1) Examples of adsorption with one and two methanethiolate molecules within the  $(2 \times 2)$  unit cell. The adsorption energies and location of the headgroup S atom are also indicated. For example,  $S_{\text{fcc}}$  corresponds to thiolate with the S headgroup at the fcc site of the substrate lattice.

For  $\text{CH}_3\text{S}$  adsorption on the clean  $\text{Ag}(111)$  surface, we also calculated the molecule-molecule interaction  $E_{\text{mol-mol}}$  as follows:

$$E_{\text{mol-mol}} = \frac{1}{n} [E_{n\text{CH}_3\text{S}/\text{Ag}}^{\text{slab}} - nE_{1\text{CH}_3\text{S}/\text{Ag}} + (n-1)E_{\text{Ag}}^{\text{slab}}],$$

where  $E_{1\text{CH}_3\text{S}/\text{Ag}}$  is the total energy of surface with a single  $\text{CH}_3\text{S}$  adsorbed molecule [e.g., the structure of Fig. 1(A1)]. According to the definition,  $E_{\text{mol-mol}}$  can be regarded as the energy required to dissociate  $E_{n\text{CH}_3\text{S}/\text{Ag}}^{\text{slab}}$  into  $n$  noninteracting  $E_{1\text{CH}_3\text{S}/\text{Ag}}$  parts. It is also defined such that a positive value

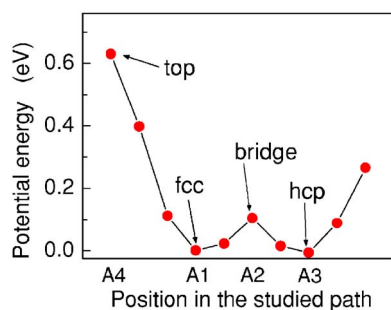


FIG. 2. (Color online) The total energy difference for a single  $\text{CH}_3\text{S}$  molecule on Ag(111) at different positions along the studied path. The studied path was indicated by the dashed line in Fig. 1(A).

indicates that the interaction is repulsive and a negative value indicates that the interaction is attractive.

The bulk equilibrium properties for Ag have been verified in a previous study.<sup>19</sup> Additional calculations of the relevant gas phase molecules  $\text{CH}_3\text{SH}$  and  $\text{CH}_3\text{S-SCH}_3$  were performed giving the geometries in reasonable agreement with experiment. In addition, test calculations have been performed to check the convergence with respect to the  $k$  point set, slab size, and vacuum thickness. We found that the adsorption energies converged to an accuracy of about 0.1 eV/molecule with respect to an eight-layer slab. We also performed test calculations using generalized gradient approximations (GGA) and found that the relative stability between structures was almost unaffected. However, the structural parameters obtained by the GGA were about 2–3 % larger than those by the LDA. We chose the LDA in this work because its structural parameters agree more with the available experimental values than the GGA's.

### III. RESULTS AND DISCUSSIONS

#### A. $\text{CH}_3\text{S}$ adsorption on the unreconstructed Ag(111) surface

As a starting point, we studied the adsorption of  $\text{CH}_3\text{S}$  on the unreconstructed Ag(111) surface using a  $(2 \times 2)$  surface unit cell. Knowledge of the adsorption site and adsorption structure is the first step towards a detailed understanding of the SAMs' structure on Ag(111). Therefore we calculated the energy profiles for a single  $\text{CH}_3\text{S}$  molecule in the  $(2 \times 2)$  surface unit cell. In the calculation, the  $\text{CH}_3\text{S}$  molecule was placed in a succession of locations. The head S atom of the  $\text{CH}_3\text{S}$  molecule interacting with the Ag(111) surface was allowed to relax only in the direction normal to the surface. The studied path was indicated by the dashed line in Fig. 1(A)—i.e., the thiolate was moved from top [Fig. 1(A4)] to fcc [Fig. 1(A1)], then over the bridge [Fig. 1(A2)] to the hcp site [Fig. 1(A3)]. The results were shown in Fig. 2. They were calculated as the total-energy difference between a  $\text{CH}_3\text{S}$  molecule at a given site and at the most stable adsorption site (i.e., the fcc site). Our results show that (i) the threefold fcc and hcp hollow sites are the most stable adsorption sites with almost the same adsorption energies and (ii) the top sites, bridge sites, or the low symmetry sites, that are intermediate between the bridge and threefold hollow sites are all less stable than the threefold hollow sites. The opti-

TABLE I. The calculated adsorption energies and surface geometries of 0.25 ML  $\text{CH}_3\text{S}$  adsorption at different surface sites on Ag(111). Here,  $\Delta E_{\text{ads}}$  denotes the relative adsorption energy difference with respect to the structure shown in Fig. 1(A1).  $d_z$  is the vertical distance between the S atom and the first surface Ag layer,  $r(\text{S-Ag})$  is the S-Ag bond distance and  $\theta$  is the tilt angle of the S-C bond away from the surface normal direction.

Adsorption site	$E_{\text{ads}}$ (eV)	$\Delta E_{\text{ads}}$ (eV)	$d_z$ (Å)	$r(\text{S-Ag})$ (Å)	$\theta$ (°)
fcc [Fig. 1(A1)]	−2.10	0.0	1.98	2.59	12.7
hcp [Fig. 1(A2)]	−2.10	0.0	1.98	2.59	12.7
Bridge [Fig. 1(A3)]	−1.99	0.11	2.02	2.52	14.8
Top [Fig. 1(A4)]	−1.46	0.64	2.33	2.43	19.0

mized atomic geometries and the adsorption energy were also listed in Table I. The bridge site is only 0.11 eV less stable than the threefold hollow sites, indicating that the adsorption potential energy surface (PES) is relatively flat. The top site is the most unfavorable adsorption site which is disfavored by about 0.64 eV than the fcc site. It is of interest to compare the results presented above with those of  $\text{CH}_3\text{S}/\text{Cu}(111)$  and  $\text{CH}_3\text{S}/\text{Au}(111)$ . The PES for  $\text{CH}_3\text{S}/\text{Cu}(111)$  was extremely shallow: the bridge site was only 0.01 eV less favorable than the fcc site, whereas the top site was 0.5 eV above the fcc site.<sup>20</sup> The PES for  $\text{CH}_3\text{S}/\text{Au}(111)$  displayed some distinctly different features: the fcc site was 0.4 eV more favorable than the bridge site, and 0.95 eV more favorable than the top site.<sup>21</sup> It has been argued that the more ionic bonding of thiolates with Cu would have a much less directional character than with gold,<sup>20</sup> qualitatively explaining the flat PES of  $\text{CH}_3\text{S}/\text{Cu}(111)$ . Accordingly, the flat PES for  $\text{CH}_3\text{S}/\text{Ag}(111)$ , which was very similar to  $\text{CH}_3\text{S}/\text{Cu}(111)$ , suggests that the thiolates-Ag bonding would have more ionic character than covalent character. This ionic bonding picture for  $\text{CH}_3\text{S}/\text{Ag}(111)$  will be confirmed from the electron density plots below. It is worth mentioning that the long-range van der Waals (vdW) interactions, which may play an important role in the SAMs formation, were not included in our calculation. However, the vdW interaction may be less strong for methanethiol than for thiolates with longer tail chains because methanethiol is the simplest alkanethiol.

To date, theoretical studies of thiolate-Ag(111) are rather limited. The adsorption energy reported by Akinaga *et al.*<sup>10</sup> using a two-layer thick cluster was calculated to be 46.94 kcal/mol (2.03 eV). The S-Ag bond length was determined to be 2.60 Å. More recently, Cometto *et al.*<sup>11</sup> obtained a value of 39.58 kcal/mol (1.72 eV) with the same cluster model and a value of 47.1 kcal/mol (2.04 eV) using a  $(\sqrt{3} \times \sqrt{3})$ -Ag(111) slab model. The S-Ag bond length was found to be about 2.555 Å. The calculation by Sellers *et al.*<sup>12</sup> reported the shortest S-Ag bond length (2.33 Å) using a cluster model at Hartree-Fock-electron correlation level. Our value for the adsorption energy (S-Ag bond length) was calculated to be 2.10 eV (2.59 Å) for the fcc site, reasonably consistent with the results of Akinaga and Cometto. The deviation of



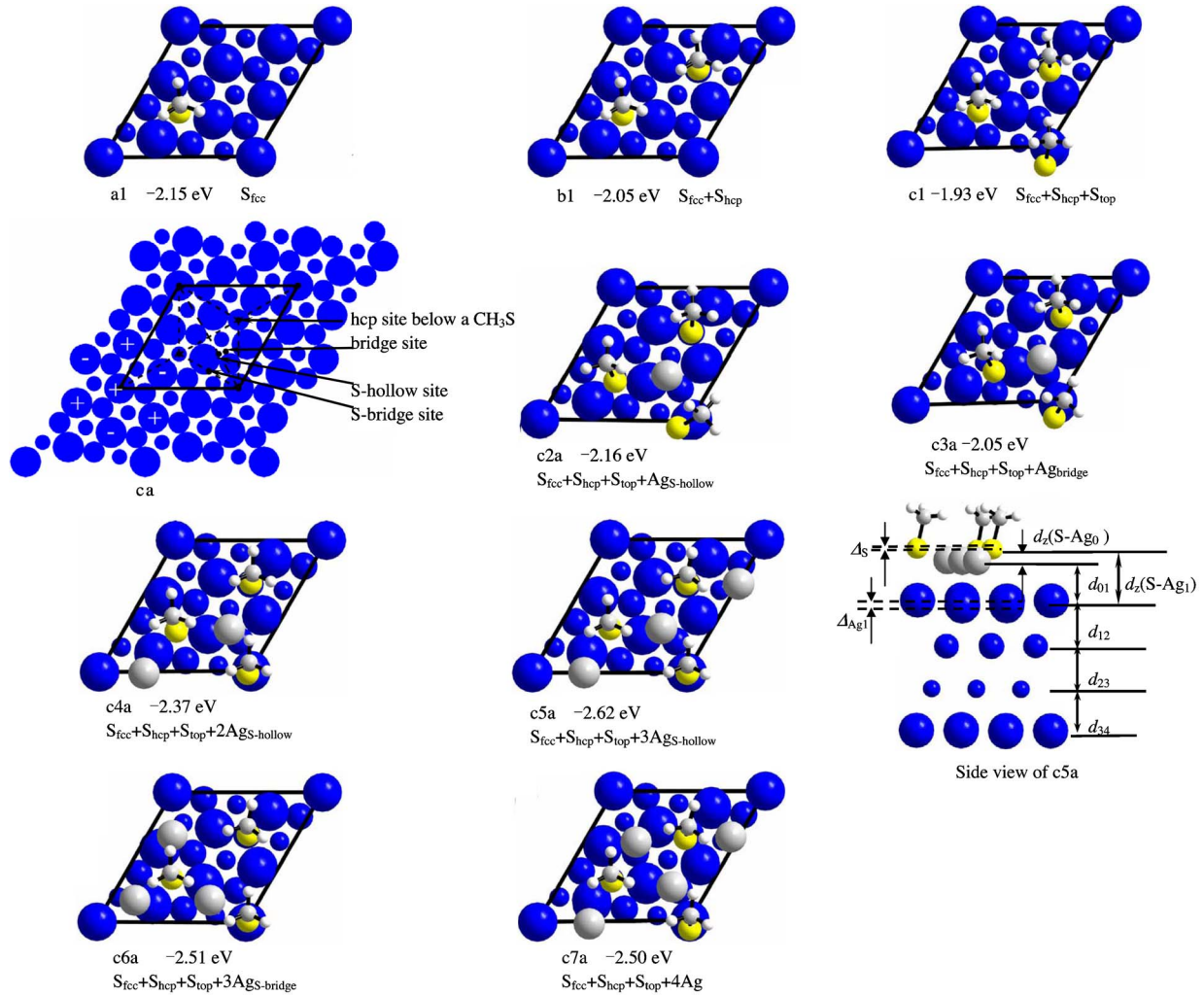


FIG. 3. (Color online) Examples of adsorption within the  $(\sqrt{7} \times \sqrt{7})R19^\circ$  surface unit cell: a1–c1 on the unreconstructed Ag(111) surface, and c2a–c7a on the reconstructed Ag(111) surface. The adsorption energies and location of the head S and Ag adatoms are also indicated. Note that some S atoms have lateral displacement from the location indicated. For reconstructed model the large gray balls denote the Ag adatoms. In ca, the S-hollow and S-bridge sites for the Ag adatoms were indicated, which assumed that three  $CH_3S$  molecules occupy the ideal top, fcc, and hcp sites, respectively, relative to the Ag substrate. The dashed lines are used to guide the eyes. The minus (plus) sign for surface Ag atoms represents the inwards (outwards) relaxation for the structure of c5a. The  $CH_3S$  and Ag adatoms produced by the periodic boundary conditions were omitted for clarity.

Sellers' results may be due to the different type of calculation used. Moreover, it was also found that the adsorption energy difference between the fcc and bridge site is small, of the order of about 0.10 eV.<sup>11</sup>

Next, we added one additional  $CH_3S$  molecule to the Ag(111) surface which corresponds to the  $CH_3S$  coverage of 0.5 ML (1.0 MLs means one  $CH_3S$  molecule per one surface Ag atom). Four adsorption sites were considered for locating the two  $CH_3S$  molecules: the fcc, hcp, bridge, and top sites. The nearest distance between two head S atoms now becomes about 2.9 Å [Fig. 1(B1)]. The fcc sites were the most stable sites with a adsorption energy of -1.21 eV [Fig. 1(B1)]. Compared to -2.10 eV for the structure of Fig. 1(A1), it can be seen that the adsorption energies for the structure of Fig. 1(B1) decrease by 0.89 eV, indicating a repulsive interaction between the  $CH_3S$  molecules. To gain deeper insight into the bonding mechanism for  $CH_3S$  adsorp-

tion on the Ag(111) surface, we also calculated the molecule-molecule interaction  $E_{mol-mol}$  for the structure of Fig. 1(B1) with respect to the structure of Fig. 1(A1), and obtained a value of 0.78 eV, suggesting that the repulsive interaction between two  $CH_3S$  molecules is the key factor of energy loss. It is worth mentioning that the difference in adsorption energy between the top and fcc site becomes less as the coverage increases. Compared to 0.64 eV/molecule at the  $CH_3S$  coverage of 0.25 ML (cf. Table I), it reduces to 0.20 eV/molecule.

### B. Interface structure of $CH_3S/Ag(111)$

As guided by the experimental results, we now use a larger surface unit cell in the calculation—i.e., a  $(\sqrt{7} \times \sqrt{7})R19^\circ$  surface unit cell. We first considered the adsorption on the unreconstructed Ag(111) surface with one, two,

and three  $\text{CH}_3\text{S}$  molecules. Structure optimizations were performed for a variety of initial geometries in order to identify the most favorable structure at given  $\text{CH}_3\text{S}$  coverages. These included geometries with different adsorption sites, different orientation of molecule, and different distance between two molecules. The respective most favorable structures are shown in Figs. 3(a1)–3(c1). The adsorption energy for one  $\text{CH}_3\text{S}$  molecule occupying the fcc site [Fig. 3(a1)] was calculated to be  $-2.15$  eV, which is  $0.05$  eV more favorable than that at  $\text{CH}_3\text{S}$  coverages of  $0.25$  ML [Fig. 1(A1)]. We also see that the overall variation in the magnitude of the adsorption energies is only  $0.22$  eV when the  $\text{CH}_3\text{S}$  coverage varies from  $1/7$  to  $3/7$  ML. Compared to the variation of  $0.89$  eV for the  $\text{CH}_3\text{S}$  coverage changing from  $0.25$  to  $0.50$  ML, it suggests that the repulsive molecule-molecule interaction for these structures becomes less. Note that the  $\text{CH}_3\text{S}$  molecule adsorbed at the top site [Fig. 3(c1)] was laterally displaced from the precise top site by about  $0.92$  Å. This is not hard to understand because the top site is the most unfavorable adsorption site on the clean Ag(111) surface (cf. Table I). Test calculations also shows that the adsorption energy decreases markedly for structures with the S-S distance of less than  $4.0$  Å. Dimerization of  $\text{CH}_3\text{S}$  on the surface—i.e., forming dimethyl-disulfide ( $\text{CH}_3\text{S-SCH}_3$ ), is energetically unfavorable [more than  $1.75$  eV unfavorable than the structure of Fig. 3(b1)].

From the results above, we found that the structure shown in Fig. 3(c1) does not correspond to the  $(\sqrt{7} \times \sqrt{7})\text{R}19^\circ$  phase found in the experiment because both the LEED and STM analyses revealed that within the  $(\sqrt{7} \times \sqrt{7})\text{R}19^\circ$  unit cell one of the  $\text{CH}_3\text{S}$  molecules occupied the top site.<sup>8</sup> In order to stabilize the  $\text{CH}_3\text{S}$  molecule adsorption at the top site, we reconstructed the Ag(111) surface by adding Ag adatoms to the surface. A number of structures containing up to four Ag adatoms were considered. We began by adding one Ag adatom to the surface. All possible adsorption sites for the Ag adatom were tested including the available fcc, hcp, bridge, and fcc (or hcp) site below a  $\text{CH}_3\text{S}$  molecule, bridge sites between two head S atoms (denoted as S bridge), and hollow site of the S layer (denoted as S hollow) [cf. Fig. 1(A) and Fig. 3(ca)]. Initially both the  $\text{CH}_3\text{S}$  molecules and the Ag adatom were placed  $3.0$  Å above the Ag substrate which is about  $0.6$  Å above the ideal layer spacing of Ag substrate. For Ag adatom adsorption at the fcc (or hcp) site below a  $\text{CH}_3\text{S}$  molecule, the  $\text{CH}_3\text{S}$  molecules were placed  $5.5$  Å above the Ag substrate. Then the whole system except the bottom two Ag layers was allowed to relax without constraint. The main results are as follows. (i) The S-hollow site is the most stable adsorption site for the Ag adatom. (ii) The Ag adatom adsorption on other sites, such as fcc, hcp, and bridge sites, tends to relax towards the S-hollow site. If the Ag adatom was constrained to relax only in direction normal to the surface plane, the bridge site [Fig. 3(c3a)] is  $0.33$  eV less stable in total energy than the S-hollow site. (iii) The fcc (or hcp) site below a  $\text{CH}_3\text{S}$  molecule is the most unfavorable adsorption site for the Ag adatom. After optimization it led to a tilt structure that was disfavored by about  $1.50$  eV in total energy than the S-hollow site. Therefore the adsorption sites below a  $\text{CH}_3\text{S}$  molecule were excluded for further consideration.

TABLE II. The main geometrical parameters in Å for the structure of Fig. 3(c5a). Here, Ag0 and Ag1 represent the Ag adatom layer and the first substrate Ag layer, respectively.  $\Delta_S$  and  $\Delta_{\text{Ag1}}$  denote the magnitude of the buckling of the S layer and of the first Ag layer, respectively.  $d_z$  and  $d_{ij}$  represent the interlayer distances while  $r(\text{S-Ag})$  denotes the S-Ag bond distances. For the interlayer distances, the center of mass of the layer is used. Numbers in parentheses correspond to bulk values, which were fixed.

	Fig. 3(c5a)	Expt. <sup>a</sup>
$\Delta_S$	0.10	0.3–0.5
$\Delta_{\text{Ag1}}$	0.30	
$d_z(\text{S-Ag0})$	0.640	$0.52 \pm 0.03$
$d_z(\text{S-Ag1})$	3.040	
$d_{01}$	2.400	
$d_{12}$	2.455	
$d_{23}$	2.425	
$d_{34}$	(2.367)	
$r(\text{S-C})$	1.839	
$r(\text{S}_{\text{top}}\text{-Ag0})$	2.676	2.70
$r(\text{S}_{\text{hcp}}\text{-Ag0})$	2.665	
$r(\text{S}_{\text{fcc}}\text{-Ag0})$	2.621	
$r(\text{S}_{\text{top}}\text{-Ag1})$	2.946	
$r(\text{S}_{\text{hcp}}\text{-Ag1})$	3.388	
$r(\text{S}_{\text{fcc}}\text{-Ag1})$	3.560	

<sup>a</sup>References 8 and 9.

We next added a second Ag adatom to the surface. All site combinations of the possible adsorption sites for the two Ag adatoms were taken into account (the same procedure was followed to simulate the adsorption of three and four Ag adatoms). The most stable structure is shown in Fig. 3(c4a). Comparing  $-2.16$  eV for the structure of Fig. 3(c2a) to  $-2.37$  eV for the structure of Fig. 3(c4a), the adsorption energies increase by about  $0.21$  eV, suggesting that the Ag adatoms can stabilize the  $\text{CH}_3\text{S}$  molecules.

For the case of three Ag adatoms, the structure of Fig. 3(c5a) turns out to be the most stable structure with an adsorption energy of  $-2.62$  eV, about  $0.69$  eV more favorable than in the case of unreconstruction [ $-1.93$  eV for the structure of Fig. 3(c1)]. Note that the energy required to form the reconstructed Ag(111) surface was not included. We also studied an ideal process of creating an Ag vacancy on the clean Ag surface. Such vacancy formation energy was calculated to be about  $0.65$  eV with respect to bulk Ag. Therefore even adding this energy cost to the adsorption energy, the structure of Fig. 3(c5a) still favors by  $0.04$  eV over the structure of Fig. 3(c1). The main feature for the structure of Fig. 3(c5a) is that all the Ag adatoms form a hexagonal commensurate structure within the  $(\sqrt{7} \times \sqrt{7})\text{R}19^\circ\text{-Ag(111)}$  surface unit cell. It should be emphasized here that the  $\text{CH}_3\text{S}$  molecule which is laterally relaxed from the top site for the structure of Fig. 3(c1) now occupies almost the precise top site (lateral relaxation less than  $0.01$  Å). If all three Ag adatoms adsorption at the S-bridge sites were not allowed to relax laterally [Fig. 3(c6a)], it was  $0.11$  eV ( $0.33$  eV in total energy) less stable than the structure of Fig. 3(c5a).

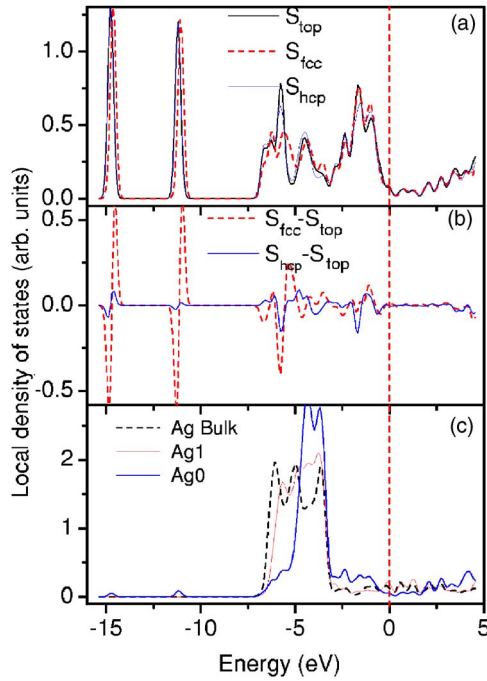


FIG. 4. (Color online) The local density of states (LDOS) for the S and Ag atoms for the structure of Fig. 3(c5a). The difference of LDOS for  $S_{fcc}$  and  $S_{hcp}$  relative to  $S_{top}$  was plotted in (b). In (c), Ag0 and Ag1 represent the Ag adatom layer and the first substrate Ag layer, respectively. The Fermi level is set to the energy zero.

Finally, we considered the adsorption of four Ag adatoms. If all four Ag adatoms occupy the S-hollow sites within the surface unit cell, the nearest distance between two Ag adatoms is about 2.6 Å while it is about 2.9 Å for the ideal substrate, indicating that the local Ag density for the Ag adatom layer is slightly larger than the substrate layer. After optimization the common feature of the resulting structures is that the Ag adatoms relaxed away from the precise S-hollow sites slightly while the  $\text{CH}_3\text{S}$  molecules also displaced slightly from the respective fcc, hcp, and top site [Fig. 3(c7a)]. Compared to four Ag adatoms occupying the precise S-hollow sites, the relaxed structure [Fig. 3(c7a)] was 0.20 eV (0.61 eV in total energy) more stable. As suggested by the NIXSW measurement, we only considered simple overlay of Ag adatoms on the clean Ag(111) surface. Therefore the possibility of reconstruction with multilayer structure can not be ruled out.

Of all the structures studied, we found that the structure shown in Fig. 3(c5a) turns out to be the most stable structure, which was also suggested to be the most possible interface structure by the NIXSW measurements.<sup>9</sup> It is worth mentioning that the stability of the most relevant structures was tested by two extra sorts of calculations. In one calculation, both the  $\text{CH}_3\text{S}$  molecules and Ag adatoms were separated 1.5 Å more apart (in  $z$  direction) from the resulting geometries. The other calculation was similar to the first one except that the  $\text{CH}_3\text{S}$  molecules or Ag adatoms were laterally displaced (in the  $xy$  direction) by about 0.15 Å. Then structural optimizations were performed again. After optimization it leads to almost the same structure as well as a few metastable structures. Therefore a proposed structural model<sup>9</sup> with the Ag adatoms lateral displacement by 0.15 Å is not appropriate. We also studied the adsorption of a single Ag adatom on the bare Ag(111) surface. The most stable adsorption sites are the fcc and hcp hollow sites. The bridge site is only 0.06 eV less favorable, indicating the PES for the Ag adatom is even more flatter than that for a  $\text{CH}_3\text{S}$  molecule (0.11 eV, cf. Table I). This implies that the positions of Ag adatom relative to the substrate are not of crucial importance and can be stabilized by the S-Ag bonding within the reconstructed layer. Namely, the interface structure of  $\text{CH}_3\text{S}/\text{Ag}(111)$  is determined to a large extent by the strength of S-Ag interaction.

The main geometrical parameters of the structure shown in Fig. 3(c5a) were given in Table II. The determined layer spacing of the adsorbate relative to the Ag adatom layer  $d_z(\text{S-Ag}_0)$  (0.640 Å) and the S-Ag bond lengths  $r(\text{S-Ag}_0)$  (2.65 Å) agree reasonably well with the experimental data ( $0.52 \pm 0.03$  Å and 2.70 Å, respectively). However, we do note that the height corrugation of the S layer  $\Delta_S$  (0.1 Å) is clearly inconsistent with experimental data (0.3–0.5 Å). Instead, we found that the corrugation of the first Ag layer  $\Delta_{\text{Ag1}}$  was quite large, about 0.3 Å. The relaxed patterns were indicated in Fig. 3(ca). Among the seven substrate Ag atoms within the surface unit cell, three Ag atoms below the  $S_{fcc}$  atom were relaxed inwards by about 0.025 Å while the other four atoms (i.e., three Ag atoms below the  $S_{hcp}$  atom and one Ag atom below the  $S_{top}$  atom) were relaxed outwards by about 0.278 Å (averaged by four Ag atoms). We note that the large corrugation of first Ag layer  $\Delta_{\text{Ag1}}$  was also found by a recent study<sup>11</sup> (about 0.31 Å using a cluster model with 25 Ag atoms). It is worth noting that in the theoretical fits for

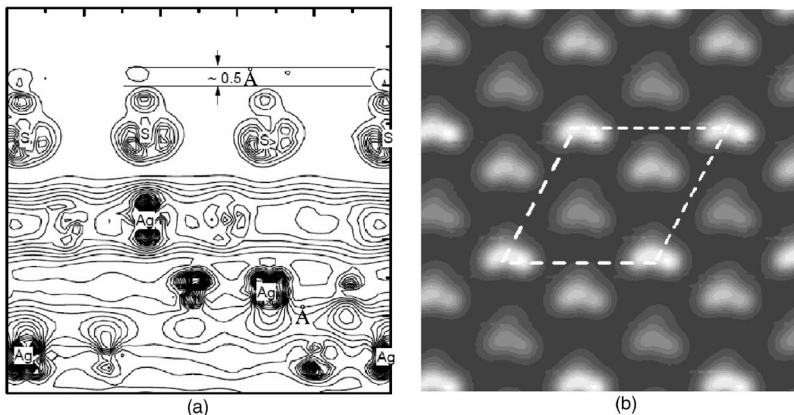


FIG. 5. Contour plots of local density of states (LDOS) at the Fermi level for the structure shown in Fig. 3(c5a). The LDOS was integrated around the Fermi level from  $-0.2$  to  $0.05$  eV. (a) and (b) represent the cross sections in planes perpendicular and parallel to the Ag(111) surface, respectively. The perpendicular plane was taken to include the S atoms while the parallel plane was cut at 1.0 Å above the outermost C atoms. The distance between contours is  $1 \times 10^{-4} \text{ e}/\text{\AA}^3$  (left) and  $1.5 \times 10^{-5} \text{ e}/\text{\AA}^3$  (right). The corrugation of LDOS and the  $(\sqrt{7} \times \sqrt{7})\text{R}19^\circ$  surface unit cell were indicated in (a) and (b), respectively.



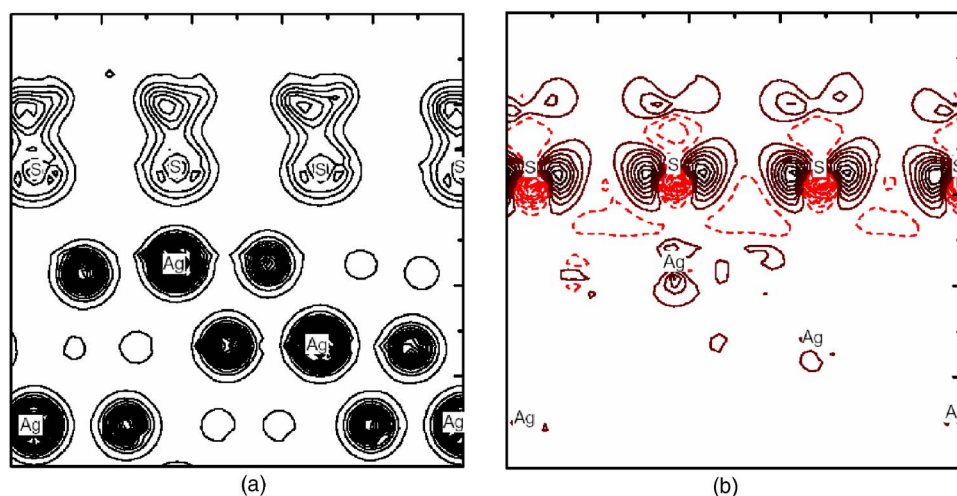


FIG. 6. (Color online) Contour plots of constant electron density in a plane perpendicular to the Ag(111) surface for the structure shown in Fig. 3(c5a): (a) total electron density, (b) electron density difference. The electron density difference is defined by  $\Delta\rho(n\text{CH}_3\text{S}/\text{substrate}) = \rho(n\text{CH}_3\text{S}) - \rho(\text{substrate})$ . The spacing between contours is  $0.4 e/\text{\AA}^3$  (left) and  $8 \times 10^{-4} e/\text{\AA}^3$  (right). Positive and negative differences are represented by solid and dashed contours, respectively.

the NIXSW measurements<sup>9</sup> a hard sphere model was adopted which used the ideal interlayer spacing of the Ag substrate—i.e., without taking into account any relaxation of the substrate. This may introduce some errors in the experimental results.

In addition, we note that the bonding environment around the S atoms is different for  $S_{\text{fcc}}$ ,  $S_{\text{hcp}}$ , and  $S_{\text{top}}$ . It may affect the strength of interaction between the head S atoms and the Ag atoms. The S-Ag bond strength can affect in turn the spatial distribution of electron density around the Fermi level. To confirm this view, we analyzed the local density of states (LDOS) for the S and Ag atoms for the structure of Fig. 3(c5a). The electronic states centered around 15.0 and 11.5 eV below the Fermi level are dominated by the S  $3s$  states [Fig. 4(a)]. The Ag  $4d$  states hybridized with S  $3p$  states, give contribution mainly in the range of  $-3.0$  to  $-7.0$  eV [Fig. 4(c)]. The LDOS around the Fermi level are dominated mainly by the S  $3p$  band. The difference of LDOS for  $S_{\text{fcc}}$  and  $S_{\text{hcp}}$  relative to  $S_{\text{top}}$  was plotted in Fig. 4(b). From this figure one can clearly see that the bonding properties are different for the three S species, though it is hardly discernable around the Fermi level.

The simulated STM image for the  $(\sqrt{7} \times \sqrt{7})\text{R}19^\circ$  SAM structure was presented in Fig. 5, which was calculated by integrating the local density of states around the Fermi level from  $-0.20$  to  $0.05$  eV. The left and right panels represent the cross sections in planes perpendicular and parallel to the Ag(111) surface, respectively. The perpendicular plane was taken to include the S atoms, while the parallel plane was cut at  $1.0 \text{ \AA}$  above the outermost C atoms. Focusing on Fig. 5(a) one can clearly see the height corrugation. Using an arbitrary spacing of  $1 \times 10^{-4} e/\text{\AA}^3$  contour the amplitude of the corrugation was estimated to be of the order of about  $0.5 \text{ \AA}$ , in reasonable agreement with the experiment (cf. Table II). Moreover, the simulated STM image [Fig. 5(b)] is qualitatively consistent with the experimental STM images,<sup>8</sup> in which one molecule in the  $(\sqrt{7} \times \sqrt{7})\text{R}19^\circ$  unit cell is imaged brighter than the other two. It confirms that the spatial distribution of electron density around the Fermi level is really different for the three  $\text{CH}_3\text{S}$  molecules though the height variation is only  $0.1 \text{ \AA}$ . We also noticed that the simulated image for  $S_{\text{hcp}}$  is slightly different from that for  $S_{\text{fcc}}$ . Such

feature can be really seen in the experimental STM images by using different tunneling voltages and currents. On the basis of the above results we concluded that the structure of Fig. 3(c5a) would be the most possible interface structure of  $\text{CH}_3\text{S}/\text{Ag}(111)$  and the height corrugation of the S layer suggested by experiment<sup>8,9</sup> is due to the electronic effects—i.e., different spatial distribution of electronic density was induced by the different S-Ag bond strength.

To further investigate the bonding mechanism for the adsorption of  $\text{CH}_3\text{S}$  molecules on the Ag(111) surface, the total and electron density difference for the structure shown in Fig. 3(c5a) were presented in Fig. 6. The electron density difference was obtained by subtracting the superposition of the electron density of the adsorption molecules  $\text{CH}_3\text{S}$  and the Ag(111) surface from that of  $\text{CH}_3\text{S}/\text{Ag}(111)$ . Figure 6(b) reveals that the electron density is depleted at the S-Ag bond close to the S atom (S  $p_z$  orbitals), while there is a slight increase in the Ag  $d_z^2$  orbitals very close to the Ag atom. Moreover, the electron density in the S  $3p_x$  ( $p_y$ )-like orbitals increases strongly, and the surface Ag  $5s$  electrons, which are in a delocalized shape, are depleted. Therefore the S-Ag bonding is essentially ionic. This is consistent with the previous calculation.<sup>10</sup> It is of interest to compare the results for  $\text{CH}_3\text{S}/\text{Ag}(111)$  presented above with those of  $\text{CH}_3\text{S}/\text{Cu}(111)$  and  $\text{CH}_3\text{S}/\text{Au}(111)$ . For the S-Au bond, it was found that the electron density increases mainly in regions halfway between the Au and S atoms, and is depleted near the Au and S atoms, revealing a covalent character.<sup>22</sup> The S-Cu bond was found to be strongly polarized with a charge accumulation near the S atom and a depletion near the Cu atom.<sup>23</sup> This is very similar to the S-Ag bonding picture described above. So the Cu-S bonding is also ionic. In fact, these noble metal-S bonding picture can be explained in terms of a simple electronegativity argument. Given the fact that Au and S are more electronegative than Cu and Ag (the Pauling electronegativity for them: Cu 1.90, Ag 1.93, Au 2.54, and S 2.58), it would result in an ionic picture in the S-Cu and S-Ag bonding, and a more covalent and directional picture in the Au-S bonding.

#### IV. SUMMARY

The adsorption of methanethiolate ( $\text{CH}_3\text{S}$ ) on the Ag(111) surface has been investigated by *ab initio* total energy calcu-

lations. Our results show that the interface structure of  $\text{CH}_3\text{S}/\text{Ag}(111)$  is determined largely by the molecule-substrate interaction—i.e., the S-Ag bonds. From our results the energetically most favorable structure was identified. The calculated structural parameters for the layer spacing of the adsorbate relative to the nearest Ag layer and the S-Ag bond lengths are in reasonable agreement with the available experimental results. However, the result of 0.10 Å for the height corrugation in the S layer is clearly inconsistent with

the experimental value of 0.3–0.5 Å. We explained this discrepancy in terms of the structural and electronic effects.

## ACKNOWLEDGMENTS

The author gratefully thanks Shu-ping Li for offering the computational facilities. The Siesta Research Group is gratefully acknowledged for providing us the SIESTA code (<http://www.uam.es/departamentos/ciencias/fismateriac/siesta/>).

- <sup>1</sup>A. Ulman, Chem. Rev. (Washington, D.C.) **96**, 1533 (1996).
- <sup>2</sup>F. Schreiber, Prog. Surf. Sci. **65**, 151 (2000).
- <sup>3</sup>H. Kondoh, M. Iwasaki, T. Shimada, K. Amemiya, T. Yokoyama, T. Ohta, M. Shimomura, and S. Kono, Phys. Rev. Lett. **90**, 066102 (2003).
- <sup>4</sup>M. G. Roper, M. P. Skegg, C. J. Fisher, J. J. Lee, D. P. Woodruff, and R. G. Jones, Chem. Phys. Lett. **389**, 87 (2004).
- <sup>5</sup>G. J. Jackson, D. P. Woodruff, R. G. Jones, N. K. Singh, A. S. Y. Chan, B. C. C. Cowie, and V. Formoso, Phys. Rev. Lett. **84**, 119 (2000).
- <sup>6</sup>S. M. Driver and D. P. Woodruff, Surf. Sci. **457**, 11 (2000).
- <sup>7</sup>S. M. Driver and D. P. Woodruff, Surf. Sci. **479**, 1 (2001).
- <sup>8</sup>M. Yu, S. M. Driver, and D. P. Woodruff, Langmuir **21**, 7285 (2005).
- <sup>9</sup>M. Yu, D. P. Woodruff, N. Bovet, C. J. Satterley, K. Lovelock, R. G. Jones, and V. Dhanak, J. Phys. Chem. **110**, 2164 (2006).
- <sup>10</sup>Y. Akinaga, T. Nakajima, and K. Hirao, J. Chem. Phys. **114**, 8555 (2001).
- <sup>11</sup>F. P. Cometto, P. Paredes-Olivera, V. A. Macagno, and E. M. Patrino, J. Phys. Chem. B **109**, 21737 (2005).
- <sup>12</sup>H. Sellers, A. Ulman, Y. Shnldman, and J. E. Eilers, J. Am. Chem. Soc. **115**, 9389 (1993).
- <sup>13</sup>D. Sanchez-Portal, P. Ordejon, E. Artacho, and J. M. Soler, Int. J. Quantum Chem. **65**, 453 (1999).
- <sup>14</sup>Reference configurations and cutoff radii ( $r_s, r_p, r_d, r_f$ ) (in a.u.) for constructing the core pseudopotentials for Ag, S, C, and H atoms used in this work: Ag  $5s^1 5p^0 4d^{10} 4f^0$  (2.46, 2.59, 2.20, 2.59); S  $3s^2 3p^4 3d^0 4f^0$  (1.39, 1.39, 1.59, 1.59); C  $2s^2 2p^2 3d^0 4f^0$  (1.25, 1.25, 1.25, 1.25); H  $1s^1 2p^0 3d^0$  (1.25, 1.25, 1.25).
- <sup>15</sup>Comparing to the following definition  $E_{ads} = n^{-1}[E_{n\text{CH}_3\text{S}/\text{Ag}}^{slab} - nE_{\text{CH}_3\text{S}} - E_{\text{Ag}}^{slab}]$ , the total energy of  $n$   $\text{CH}_3\text{S}$  was used in Eq. (1). Therefore the molecule-molecule interaction energy is not included.
- <sup>16</sup>C. Masens, M. J. Ford, and M. B. Cortie, Surf. Sci. **580**, 19 (2005).
- <sup>17</sup>P. Valiron and I. Mayer, Chem. Phys. Lett. **275**, 46 (1997).
- <sup>18</sup>S. B. Boys and F. Bernardi, Mol. Phys. **19**, 533 (1970).
- <sup>19</sup>Guo-min He, Phys. Rev. B **73**, 035311 (2006).
- <sup>20</sup>M. Konôpka, R. Rousseau, I. Štich, and D. Marx, Phys. Rev. Lett. **95**, 096102 (2005).
- <sup>21</sup>Y. Yourdshahyan, H. K. Zhang, and A. M. Rappe, Phys. Rev. B **63**, 081405(R) (2001).
- <sup>22</sup>L. M. Molina and B. Hammer, Chem. Phys. Lett. **360**, 264 (2002).
- <sup>23</sup>A. Ferral, P. Paredes-Olivera, V. A. Macagno, and E. M. Patrino, Surf. Sci. **525**, 85 (2003).